

Research on the ions' axial temperature of a sympathetically-cooled $^{113}Cd^{+}$ ion crystal

Nong-Chao Xin(辛弄潮), Sheng-Nan Miao(苗胜楠), Hao-Ran Qin(秦浩然), Li-Ming Guo(郭黎明), Ji-Ze Han(韩济泽), Hua-Xing Hu(胡华星), Wen-Xin Shi(施文心), Jian-Wei Zhang(张建伟), and Li-Jun Wang(王力军)

Citation: Chin. Phys. B, 2021, 30 (**11**): 113701. DOI: 10.1088/1674-1056/abe379
Journal homepage: http://cpb.iphy.ac.cn; http://iopscience.iop.org/cpb

What follows is a list of articles you may be interested in

Numerical analysis of motional mode coupling of sympathetically cooled two-ion crystals

Li-Jun Du(杜丽军), Yan-Song Meng(蒙艳松), Yu-Ling He(贺玉玲), and Jun Xie(谢军)
Chin. Phys. B, 2021, 30 (**7**): 073702. DOI: 10.1088/1674-1056/abfc3e

Setup of a dipole trap for all-optical trapping

Miao Wang(王淼), Zheng Chen(陈正), Yao Huang(黄垚), Hua Guan(管桦), and Ke-Lin Gao(高克林)
Chin. Phys. B, 2021, 30 (**5**): 053702. DOI: 10.1088/1674-1056/abd767

Optimization of endcap trap for single-ion manipulation

Yuan Qian(钱源), Chang-Da-Ren Fang(方长达人), Yao Huang(黄垚), Hua Guan(管桦), Ke-Lin Gao(高克林)
Chin. Phys. B, 2018, 27 (**6**): 063701. DOI: 10.1088/1674-1056/27/6/063701

Quantitative evaluation of space charge effects of laser-cooled three-dimensional ion system on a secular motion period scale

Li-Jun Du(杜丽军), Hong-Fang Song(宋红芳), Shao-Long Chen(陈邵龙), Yao Huang(黄垚), Xin Tong(童昕), Hua Guan(管桦), Ke-Lin Gao(高克林)
Chin. Phys. B, 2018, 27 (**4**): 043701. DOI: 10.1088/1674-1056/27/4/043701

An optimized ion trap geometry to measure quadrupole shifts of $^{171}Yb+$ clocks

N Batra, B K Sahoo, S De
Chin. Phys. B, 2016, 25 (**11**): 113703. DOI: 10.1088/1674-1056/25/11/113703

Research on the ions' axial temperature of a sympathetically-cooled $^{113}Cd^{+}$ ion crystal*

Nong-Chao Xin(辛弄潮)[1], Sheng-Nan Miao(苗胜楠)[1], Hao-Ran Qin(秦浩然)[1,2], Li-Ming Guo(郭黎明)[1], Ji-Ze Han(韩济泽)[1,2], Hua-Xing Hu(胡华星)[1], Wen-Xin Shi(施文心)[1], Jian-Wei Zhang(张建伟)[1,†], and Li-Jun Wang(王力军)[1,2]

[1] *State Key Laboratory of Precision Measurement Technology and Instruments, Department of Precision Instruments, Tsinghua University, Beijing* 100084, *China*

[2] *Department of Physics, Tsinghua University, Beijing* 100084, *China*

(Received 22 March 2021; revised manuscript received 18 May 2021; accepted manuscript online 20 May 2021)

Molecular dynamics simulation of a sympathetically-cooled $^{113}Cd^{+}$ ion crystal system is achieved. Moreover, the relationship between ions' axial temperature and different electric parameters, including radio frequency voltage and end-cap voltage is depicted. Under stable trapping condition, optimum radio frequency voltage, corresponding to minimum temperature and the highest cooling efficiency, is obtained. The temperature is positively correlated with end-cap voltage. The relationship is also confirmed by a sympathetically-cooled $^{113}Cd^{+}$ microwave clock. The pseudo-potential model is used to illustrate the relationship and influence mechanism. A reasonable index, indicating ions' temperature, is proposed to quickly estimate the relative ions' temperature. The investigation is helpful for ion crystal investigation, such as spatial configuration manipulation, sympathetic cooling efficiency enhancement, and temporal evolution.

Keywords: ion temperature, sympathetic cooling, electric parameters, microwave clock

PACS: 37.10.Ty, 37.10.Rs, 37.90.+j, 31.15.xv **DOI:** 10.1088/1674-1056/abe379

1. Introduction

Trapping and cooling ion technique plays an important role in precision measurement field, including but not limited to frequency standards, quantum information processing, and chemical reactions. This technique is employed to acquire long-term, stable, and cold (milli-Kelvin) ion crystal. Especially, frequency standards based on ion traps and Doppler laser cooling technology demonstrate great potential in the application of time-keeping,[1] space navigation,[2,3] and deep-space exploration.[4] Among the ion cooling techniques, sympathetic cooling technology is a technique that indirectly cools another type of particles on the basis of laser cooling of one type of particles.[5,6] Therefore, the transition spectrum of atoms, ions, and molecules cooled by sympathetic cooling technology can be measured more accurately. Because only the coolant particles should be cooled by laser, the particles of similar mass can be effectively cooled through the interaction between the particles. The sympathetic-cooling technology is effective for almost all particles, and significantly important in the precise measurement of particle spectrum and the study of particle properties.[7,8] Through sympathetic cooling technique, microwave clock based on sympathetically-cooled $^{113}Cd^{+}$ ions[9] has been proven to be conducive to overcoming limits, including Dick effect and second-order Doppler frequency shift (SODFS), which result from the dead time of laser cooling process and rise in temperature during the clock interrogation, respectively.[10,11]

Study has revealed that for the sympathetically-cooled ion crystal, trapped in the linear Paul trap, there exists a complex relationship between the electric parameters, including RF (radio frequency) voltage and end-cap voltage, and the temperature of ions.[9] To study the sympathetic cooling efficiency and the ion crystal temperature, we constructed an MD (molecular dynamics) simulation model of a sympathetically-cooled $^{113}Cd^{+}$ ion crystal, in which $^{40}Ca^{+}$ ions were used as the coolant to sympathetically cool a large $^{113}Cd^{+}$ cloud. Furthermore, both types of ions are trapped in a linear Paul trap. By applying MD simulation, detailed information of any particular ion, including but not limited to ions' velocity and location distribution, temperature, and evolution of secular motion together with micro-motion can be acquired reasonably and accurately.[12,13] After defining some parameters, such as ions' mass-to-charge ration, ions' quantity and potential applied on trap ions, the process of ion generating, trapping and sympathetic cooling can be simulated properly. Moreover, the pseudo-potential approximation model[14] is adopted to define motion modes of ions, and it clearly explains spatial configuration transformation and temporal evolution of the simulated three-dimensional (3D) sympathetically-cooled ion system under different voltages.

*Project supported by the Beijing Natural Science Foundation (Grant No. 1202011), the Tsinghua University Initiative Scientific Research Program, the National Natural Science Foundation of China (Grant No. 12073015), and the National Key Research and Development Program of China (Grant No. 2016YFA0302101).

†Corresponding author. E-mail: zhangjw@tsinghua.edu.cn

© 2021 Chinese Physical Society and IOP Publishing Ltd

For the ion crystal system we built, the optimum radio frequency (RF) voltage amplitude (about 260 V), corresponding to minimum temperature, was discovered. Before the optimum RF voltage, ions' axial temperature is negatively correlated with the RF voltage. While after the optimum RF voltage, ions' axial temperature experiences a steady escalation with the increasing of RF voltage. The axial temperature is positively correlated with the end-cap voltage. The change trends of ion temperature vs. the RF voltage and the end-cap voltage are consistent with the experimental results. We further proposed a simple method to estimate the axial temperature trend while tuning the voltages by a key index (see in Eq. (9)), which is determined by secular motion amplitude, average position, and $q_{x,y}$ (defined in Eq. (3)).

2. MD simulation and verifications

2.1. MD simulation model

Our MD simulation is based on Newton's classical mechanics. The force analysis of ions is the basis for molecular dynamics simulation. The i-th ion trapped in the ion trap is affected by the following four forces: (i) trapping force of the potential field $\boldsymbol{F}_i^{\text{trap}}$, (ii) interaction force with all other ions $\boldsymbol{F}_i^{\text{Coulomb}}$, (iii) random force $\boldsymbol{F}_i^{\text{stochastic}}$, and (iv) laser force $\boldsymbol{F}_i^{\text{laser}}$. Then the dynamic equation of a single ion can be expressed as

$$\begin{aligned} m_i\ddot{\boldsymbol{r}}_i &= \boldsymbol{F}_i(\boldsymbol{r}_1,\ldots,\boldsymbol{r}_{\text{LC+SC}},\boldsymbol{v}_1,\ldots,\boldsymbol{v}_{\text{LC+SC}},t) \\ &= \boldsymbol{F}_i^{\text{trap}} + \boldsymbol{F}_i^{\text{Coulomb}} + \boldsymbol{F}_i^{\text{stochastic}} + \boldsymbol{F}_i^{\text{laser}}, \end{aligned} \tag{1}$$

where ion number $i = 1,\ldots,N_{\text{LC}},\ldots,N_{\text{LC+SC}}$. N_{LC} represents the number of direct laser cooling ions (Ca^+) and N_{SC} represents the number of sympathetically-cooled ions (Cd^+).

After applying the voltage to the electrodes, within the defined coordinate system shown in Fig. 1, the electric potential in the trap and the trapping force can be expressed as

$$\begin{aligned} \boldsymbol{F}_i^{\text{trap}} &= -Q\nabla\psi = -Q\nabla\psi_{(x,y,z,t)} \\ &= -Q\nabla\left[\frac{V_{\text{rf}}\cos(\Omega t)}{2{r_0}^2}\left(x^2-y^2\right)\right. \\ &\quad \left.+\frac{\kappa U_{\text{end}}}{{z_0}^2}\left(z^2-\frac{(x^2+y^2)}{2}\right)\right], \end{aligned} \tag{2}$$

where Ω is the frequency of RF voltage and κ is the axial equivalent geometric factor, decided by the geometry of the trap and distance between two endcaps z_0. In our experiment, COMSOL software is used to construct the trap model. By setting different voltages, we fitted the corresponding trap potential, and then obtained the κ coefficient by fitting analysis. κ was set to 0.049.

The random collision force $\boldsymbol{F}_i^{\text{stochastic}}$ (Ref. [15]) and the laser force $\boldsymbol{F}_i^{\text{laser}}$ (Ref. [12]) have already been described at Ref. [10]. The evolution process uses the Leapfrog algorithm,[1,16,17] which is a second-order stable and time reversible algorithm. In addition, the choice of time step is critical in molecular dynamics simulation; it is appropriate to include dozens to one hundred time steps in an RF cycle. The time step of the model built in this article is selected as 5 ns, 1/100 of the RF cycle, and it ensures the stability of the algorithm and simultaneously guarantees the accuracy of the calculation. The time step can be changed artificially in the simulation program.

The cardinal parameters of the simulated linear Paul trap are depicted in Fig. 1.[19] Our trap is composed of four three-section cylindrical copper electrodes. The diameter of each electrode is 14.2 mm, and the shortest distance between the electrodes and the ion trap center is 6.2 mm. To trap ions in the axial direction, the end-cap voltage (U_{end}, direct current voltage) is applied on the adjacent section (A and C parts) of all electrodes. Meanwhile, to achieve confinement of ions in the radial direction, RF voltage ($U_{\text{rf}} = (V_{\text{rf}}/2)\cos\Omega t$), frequency fixed at 2.06 MHz, is assigned to the central section (B part) of electrodes 2 and 4, and the central section of electrodes 1 and 3 is well grounded. The adjustment range of amplitude of RF voltage is 150 V–500 V, and the output amplitude of end-cap voltage can be varied from 0 V to 100 V. The cooling laser and the probe laser are shined on ions in the direction of the axial of trap. Thus, axial temperature of the ion cloud is investigated in the following analysis.

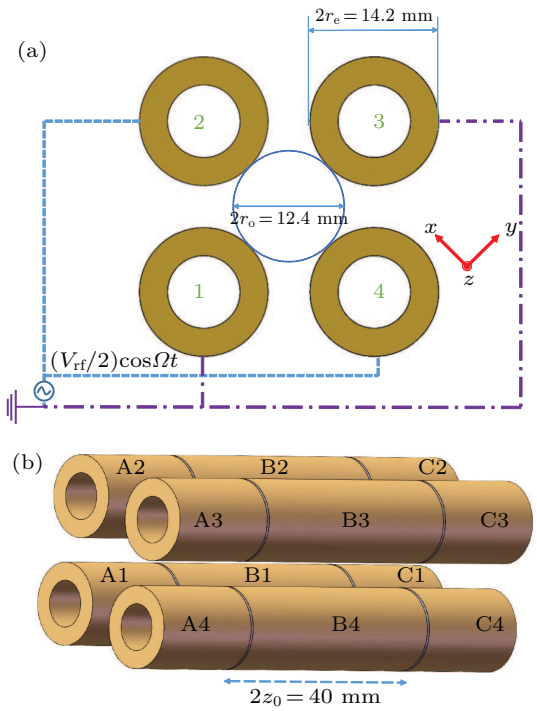


Fig. 1. Sketch of linear Paul trap: (a) axial view and (b) side view. The origin of z axis of our coordinate is centered between endcaps.

2.2. Verifications

Before the investigation, our simulation program was validated by comparing the simulated results to the analytic and

experimental results. These tests allows detection if modifications introduce errors; thus, ensuring correctness of the further illustrations.

By using pseudo-potential approximation, motion of a single ion can be depicted as[20,21]

$$r_i = r_{0i}\cos(\omega_i t)\left(1+\frac{q_i}{2}\cos(\Omega t)\right), \tag{3}$$

where $\boldsymbol{r} = r_x\hat{x} + r_y\hat{y} + r_z\hat{z}$ determine ions' triaxial position in the coordinate system defined in Fig. 1, and

$$a_z = 2a_x = 2a_y = -\frac{4Q\kappa U_{\text{end}}}{m\Omega^2 {z_0}^2},$$
$$q_x = -q_y = \frac{QV_{\text{rf}}}{m\Omega^2 {r_0}^2}, \quad \omega_x = \frac{\Omega}{2}\sqrt{a_x + \frac{{q_x}^2}{2}},$$
$$\omega_y = \frac{\Omega}{2}\sqrt{a_y + \frac{{q_y}^2}{2}}, \quad \omega_z = \frac{\Omega}{2}\sqrt{a_z}.$$

In radial direction, the motion of one single ion is separated into a secular motion at frequency $\omega_{i,i=x,y}$ and a swift 'micromotion' at frequency Ω. In axial direction, the single ion only oscillates at frequency ω_z.

Apparently, these frequencies depend on end-cap and RF voltages. Motion of one ion is simulated by our program, and the oscillation frequencies are extracted along each axis, as demonstrated in Fig. 2(a), which validates the correctness of end-cap and RF voltages.

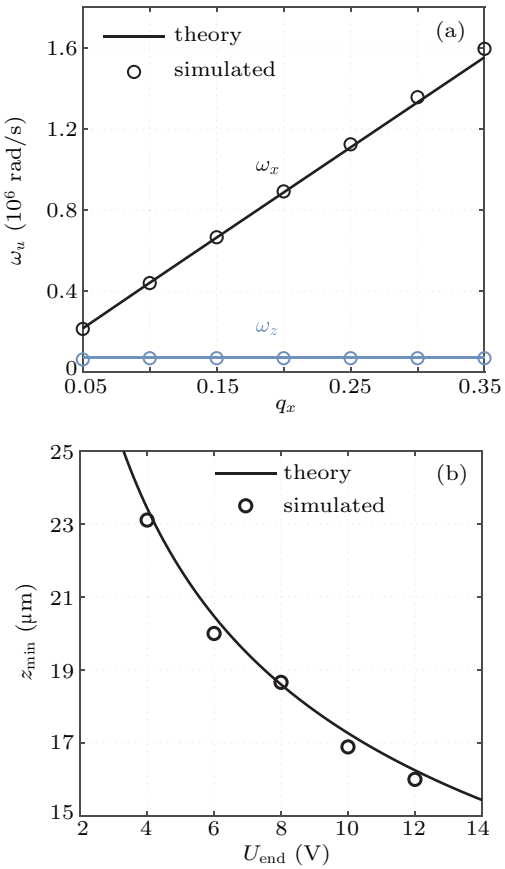


Fig. 2. (a) Oscillation frequencies extracted from simulation of one single ion. The frequencies are all from the Fourier component with the largest amplitude. (b) Relationship between minimum separation of ions and U_{end}. The number of ions is 64.

Moreover, when the number of ions is sufficiently small that all ions are aligned through the z axis, the distance between N ions (quantity of electric charge of each ion is Q and m is the ion mass) will increase away from the center of z axis. The minimum separation between ions is expressed as[22]

$$z_{\min} \approx \frac{2.018}{N^{0.559}}\left(\frac{Q^2}{4\pi\varepsilon_0 m{\omega_z}^2}\right). \tag{4}$$

Figure 2(b) shows the minimum simulated separation and the value predicted by theory. Because the simulated ions experience forces, including the voltage confinement along z axis and the Coulomb force from the other ions, simulation of the minimum separation of ions tests the realization of both the Coulomb force and voltage confinement.

The forces experienced by ions decide the spatial configuration of ion crystal. In our experiment, an explicit ion crystal picture of Ca^+ was obtained by an EMCCD (electron-multiplying charge coupled device). Under our experimental settings, we estimated the number of ions based on the size of the ion cloud,[23] and after repeated release of trapped ions, we selected the experimental results of approximately $1.9\,(0.5)\times10^4$ Ca^+ ions as the correctness verification of the simulation model. The corresponding ion number was calculated as $1.9\,(0.5)\times10^4$. Figure 3 shows pictures of ion crystal obtained from the experiment and simulation, verifying that our simulation results are consistent with the real experimental results.

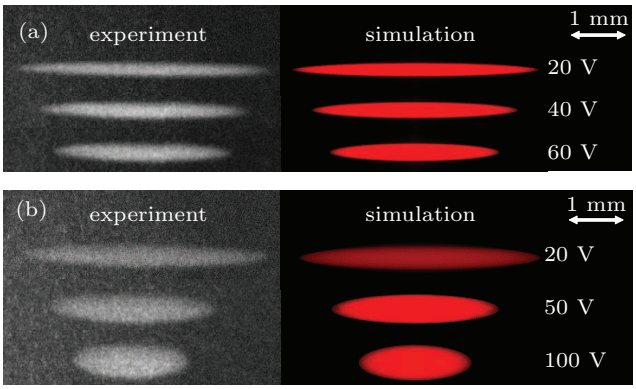


Fig. 3. Ca^+ ion crystal obtained from experiment and simulation at different RF voltages and end-cap voltages. (a) $V_{\text{rf}} = 400$ V. (b) $V_{\text{rf}} = 240$ V. The number of Ca^+ is $1.9\,(0.5)\times10^4$.

3. Relationship between ions' temperature and electric parameters

3.1. Simulation results

As shown in Fig. 4, increasement of RF and end-cap voltages change the spatial configuration of ion crystal. Typically, increasing RF voltage and end-cap voltage lead to substantial compression and extension on the radial distribution of the ion system, respectively. Because the effect of laser force is significant,[24–26] during the simulation process, the laser force is set as a constant value, verified by Subsection 2.2.

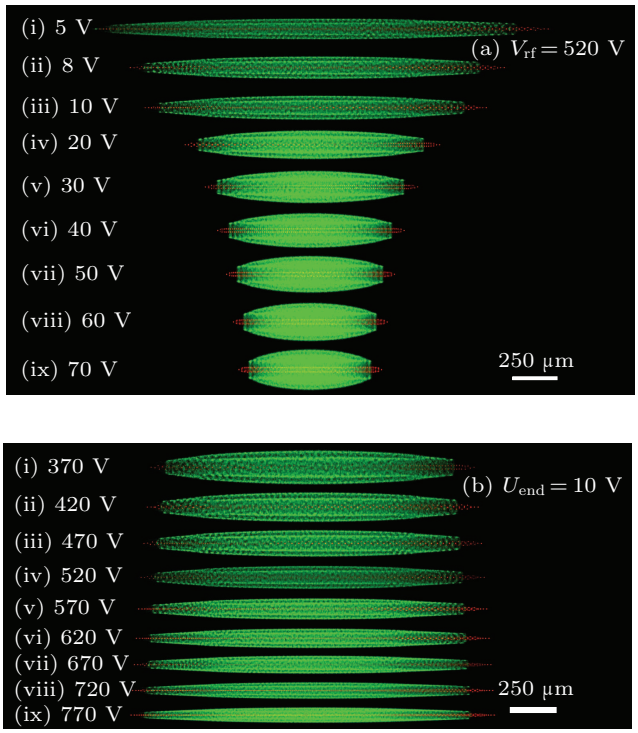


Fig. 4. Spatial configuration of ion crystal obtained from simulation. (a) Spatial configuration of ion crystal cloud changes with end-cap voltage at $V_{rf} = 520$ V. (b) Spatial configuration of ion crystal cloud changes with RF voltage at $U_{end} = 10$ V. Red dots represent the ions of Ca^+ and green dots represent the ions of Cd^+. The ion numbers of Ca^+ and Cd^+ are 192 and 960, respectively.

Note that although reducing the end-cap voltage will lead to the decline of ion temperature, considering the actual situation that the ions should be stably trapped, the end-cap voltage should have a lower limit. In our previous sympathetic cooling experiment,[27] we found that when the end-cap voltage is lower than 10 V, the ion loss rate increases; thus, we usually set the end-cap voltage above 10 V. The specific lower limit of the end-cap voltage is related to the specific trap parameters, vacuum degree, laser parameters, and other experimental conditions.

Theoretically, the temperature of the ions in the thermal equilibrium state affected by the voltages can be explained by the RF heating effect.[21,28,29] The RF heating effect is correlated with the oscillation amplitude and frequency of the ions. Through the image obtained from the simulation (see in Fig. 4), it can be observed that when the end-cap voltage increases and the RF voltage decreases, more ions are arranged outside the central axis, which means that oscillation amplitude is amplified. Further, it is verified that the frequency of the motion is affected by the voltages. When the oscillation amplitude and the movement frequency both affected by the voltages, the specific changes of the ion temperature need to be discussed in detail. In Subsection 3.2, motion equation under the pseudo-potential model is applied to provide a more reasonable and clear explanation.

Figure 5 demonstrates the specific ions' axial temperature at different RF voltage and end-cap voltage. According to the simulation results, the optimum RF voltage corresponding to the lowest temperature is approximately 520 V. Still, before the optimum RF voltage, the temperature decreases with the increasement of RF voltage, and after the optimum voltage, the temperature increases with the increasing of RF voltage. Furthermore, the end-cap voltage and temperature are positively correlated.

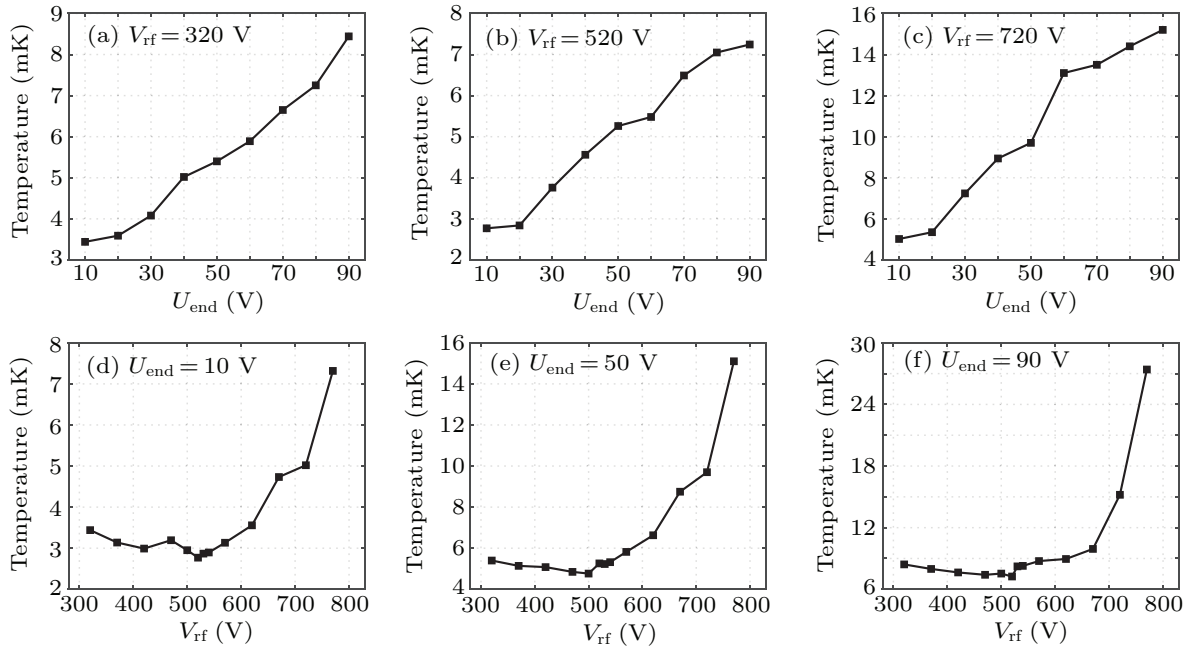


Fig. 5. Temperature from simulation: (a) axial temperature at different end-cap voltages with $V_{rf} = 320$ V; (b) axial temperature at different end-cap voltages with $V_{rf} = 520$ V; (c) axial temperature at different end-cap voltages with $V_{rf} = 720$ V; (d) axial temperature at different RF voltages with $U_{end} = 10$ V; (e) axial temperature at different RF voltages with $U_{end} = 50$ V; (f) axial temperature at different RF voltages with $U_{end} = 90$ V. The ion numbers of $^{40}Ca^+$ and $^{113}Cd^+$ are 192 and 960, respectively.

3.2. Energy and temperature

The motion of one single ion can be well expressed by Eq. (3). When considering large-scale ion cloud trapping, modifications and assumptions should be mentioned. Owing to the Coulomb force, more ions will distribute around the z axis. Average position of ions are placed to (r_{1x}, r_{1y}, r_{1z}), which causes 'excess micro-motion'.[21] Thus the motion of ions is modified as

$$r_i = [r_{1i} + r_{0i}\cos(\omega_i t)]\left(1 + \frac{q_i}{2}\cos(\Omega t)\right). \tag{5}$$

The modified equation motion of ions indicates that ions oscillate at an average position with an amplitude of $\frac{1}{2}r_{1i}q_{i,i=x,y,z}$. Equation (5) is based on the pseudo-potential approximation and can describe the main motion modes of ions.

To illustrate the energy change of ion cloud clearly, it is better to first fully describe the ion motion modes. According to Eq. (5), the one-dimensional motion of the ions can be mainly described by the superposition of the secular motion and the micro-motion. However, considering that the ions move in three-dimensional (3D) space, the movement of ions in the 3D direction will be coupled with each other, resulting in more complicated ion movement patterns. Therefore, although the motion modes of ions become complex due to mutual coupling, they are result of combined secular motion and micro-motion. By calculating the kinetic energy of the ions in the micro-motion and secular motion modes, the overall energy of the ions can be reflected. In addition, due to the high coupling of ion motion modes, the energies of ions in the three degrees of freedom are positively correlated. Therefore, we can use the motion equation of the ion in one direction to estimate the total energy of the ion in the complex motion within the three-dimensional space.

For a 3D ion system, interaction among ions leads to motion and energy coupling under different dimensions. Thus, it is assumed that ions' triaxial energy is in the same order of magnitude and positively correlated:

$$E_z \propto E_x \propto E_y. \tag{6}$$

Furthermore, according to our simulation, ions' axial micro-motion mainly results from motion coupling among different dimensions and is less affected by the RF driving field, while ions' radial motion is a direct superposition of the micro-motion and secular motion.[30] To analyze the energy and temperature evolution of the ions more comprehensively, we used the axial motion equation of the ions, obtained from the equivalent harmonic pseudo-potential approximation, to figure out the energy and temperature of ions in the 3D sympathetically-cooled ion system.

Averaged over a period of secular motion, the kinetic energy of ions in x direction can be obtained as[21]

$$E_x = \frac{1}{2}m\langle \dot{r}_x^2 \rangle = \frac{m\Omega^2}{16}(a_x {r_{0x}}^2 + {r_{0x}}^2 {q_x}^2 + {r_{1x}}^2 {q_x}^2). \tag{7}$$

Typically, $a_{i,i=x,y}$ is significantly smaller than $q_{i,i=x,y}$, and quite close to 0. The energy can then be modified as

$$E_x \approx \frac{m\Omega^2}{16}{q_x}^2({r_{1x}}^2 + {r_{0x}}^2). \tag{8}$$

What is more, the temperature of the ions can be explained macroscopically as the average value of the sum of ions' kinetic energy

$$\begin{aligned} T_z &\propto \frac{1}{N}\sum_{i=1}^{N} E_{zi} \propto \frac{1}{N}\sum_{i=1}^{N} E_{xi} \\ &\approx \frac{m\Omega^2}{16N}{q_x}^2 \sum_{i=1}^{N}({r_{1xi}}^2 + {r_{0xi}}^2), \end{aligned} \tag{9}$$

where the number of ions is N, r_{1xi} is the average position of i-th ion along x direction, indicating the deviation of ions towards the central axis.

By using Eq. (9), the evolution process of sympathetically cooled ions' temperature and energy under different voltages, portrayed by Fig. 5, can be distinctly described:

According to Eq. (9), energy and temperature of ions in a 3D ion sympathetic cooling system are positively correlated with the amplitude of secular motion, average position of ions and $q_{x,y}$. On the one hand, by increasing the RF voltage, the spatial configuration is compressed, indicating the decline of secular motion amplitude and average position value. Thus, increasing $q_{x,y}$ (determined by increasing RF voltage) and decreasing secular motion amplitude together with average position value imply the minimum ion energy and temperature at a certain RF voltage. On the other hand, because increasing end-cap voltage amplifies the secular motion amplitude and average position, while have slight influence on $q_{x,y}$,[20] ions' temperature and energy are reasonably positively correlated with the end-cap voltage.

Moreover, it is assumed that ion crystal configuration is determined by all ions' motion amplitude and average position. Thus, the configuration can microscopically represent the average of square of the secular motion amplitude and average position. In this study, we chose the maximum radial width of ion crystal as the cardinal parameter of the ion crystal configuration. Thereafter, the axial temperature was microscopically evaluated by a new index u:

$$u = {q_x}^2 {R_{\rm sc}}^2, \tag{10}$$

where $R_{\rm sc}$ represents the maximum radial width of sympathetically cooling ion crystal (Cd^+) in our simulation.

The dimension of index u is square of meter. It contains important information that affect ions energy, including electric parameters and oscillation amplitude. It reflects the energy and spatial configuration change under different voltages. Under a specific ion crystal trapped in linear Paul trap, it helps to estimate relative temperature value conveniently and quickly.

Further, it allows us to measure R_{sc} and determine corresponding u through the simulation output. The exact calculation results are depicted as follows:

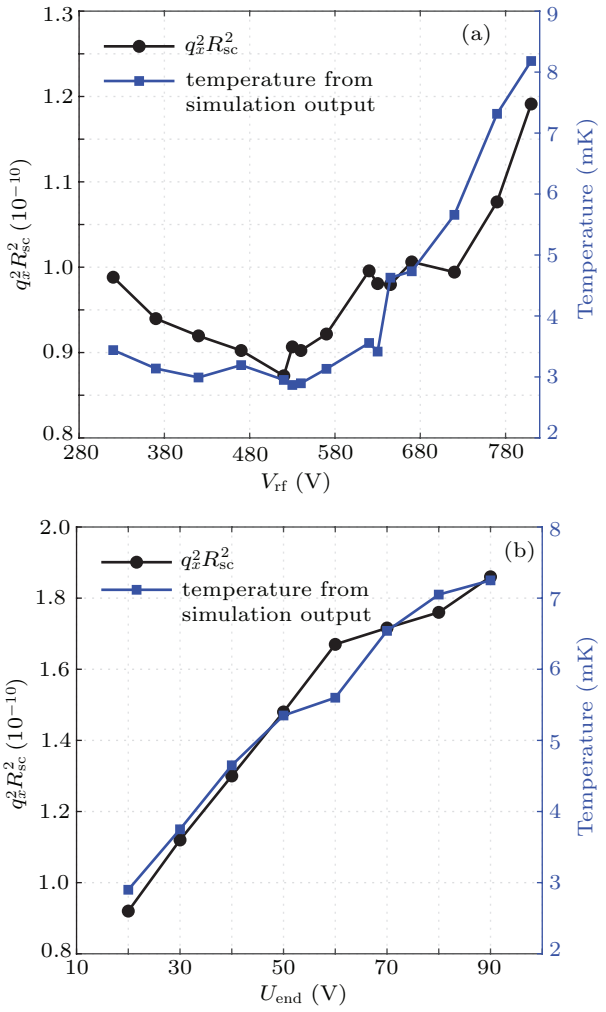


Fig. 6. Index to evaluate temperature of sympathetic cooling ions. (a) Temperature from simulation and the index at different RF voltages with $U_{end} = 10$ V. (b) Temperature from simulation and the index at different end-cap voltages with $V_{rf} = 520$ V. The number of ions is the same as that in Fig. 4. Discontinuous point data around 620 V are a phenomenon of random fluctuations of macroscopic physical quantities. Under the thermal equilibrium state, the macroscopic physical quantities of ions such as temperature, velocity, and energy, should own certain degree of random fluctuations. This type of random fluctuation becomes more significant when the voltage parameter changes slightly.

The temperature change trend reflected by the index u is consistent with the simulation results, especially when the temperature reaches at a minimum with $V_{rf} = 520$ V.

Though the temperature evolution process, as discovered and illustrated by MD simulation and pseudo-potential model, we confirmed the RF optimum voltage (around 520 V) through a sympathetically-cooled $^{113}Cd^+$ ion microwave clock (shown in Fig. 7).[26]

Detailed experimental setup and temperature measurement method can be found in Ref. [27]. The temperature evolution processes are experimentally measured by evaluating the Doppler broadening owing to ion motion of the $5p^2P_{3/2}F = 2, m_F = 2 \rightarrow 5s^2S_{3/2}F = 1, m_F = 1$ transition. At the published studies, we estimated the loss of ions based on the intensity of the fluorescence radiation of the ions. The fitted fluorescence decay curve is an exponential decay curve, and the time constant is approximately 84 h. Thus, it is reasonable to assume that the number of ions remains unchanged within 1 hour, and the experimental error caused by the loss of ions can be ignored.[27]

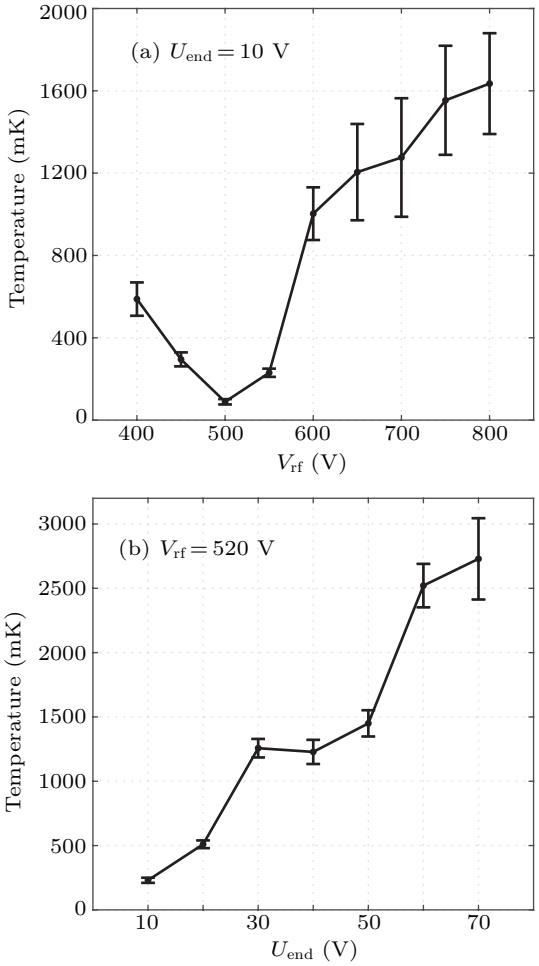


Fig. 7. Influence of electric parameters on ions' axial temperature. (a) Corresponding temperature at different RF voltages with $U_{end} = 10$ V. (b) Corresponding temperature at different end-cap voltages with $V_{rf} = 520$ V. The temperature data of $^{40}Ca^+$ and $^{113}Cd^+$ ion crystals under sympathetic cooling situation are adopted from Ref. [26].

Though the changing trend obtained from simulation and experiment is consistent, some details are slightly different. We believe that the main reasons for the inconsistency of the simulation results, experimental results, and theoretical calculation results are as follows:

(i) In the experiment, the potential of the ion trap is not a perfect quadruple potential, which will cause additional RF heating.

(ii) The number of ions in the experiment is significantly higher than the simulation calculation. It is believed that even under the same electrical parameters, the ion cloud size formed by different numbers of ions changes notably. Increasing number of ions leads to expansion of the ion cloud, which implies

an intensified RF heating. Thus, the temperature measured through the experiment is much higher than that of the simulation.

(iii) Theoretical calculation of the relative temperature of the ion requires the identification of the specific size of the ion cloud. Although the ion cloud image captured by the EMCCD and obtained by the simulation result are notably clear, there are still errors in determining the size of the ion cloud.

The sympathetic cooling system simulated in this study is aimed at the sympathetic cooling of metal ions, and distinguished with sympathetic cooling system of highly charged ions, atoms, and molecular ions. For metal ions of different masses, although their spatial configuration is different, their motion modes are still superposition of micro-motion and secular motion. Then the influencing factors of ions' energy in the linear trap should be consistent. The index u provides us a convenient method to estimate the ions' temperature changing trend in experiment, which avoids scanning probe laser frequency to measure the Doppler broadening of a transition.

4. Conclusion

In this paper, we simulated a sympathetically-cooled ion system. The MD simulation results offered detailed information of any given ion at a certain time, based on which axial temperature of the ion crystal under different voltages was calculated.

Using the pseudo-potential approximation model, key factors, composed of secular motion amplitude, average position and $q_{x,y}$, affecting ions' temperature and energy were elaborated. RF and end-cap voltages were found to have influence on these factors and can change the ions' axial temperature accordingly.

Based on the key factors, index u, a square of the product of q and R_{sc}, is able to help us determine ions' temperature relatively and quickly. The temperature change, indicated by the index, is consistent with the simulation result, and both are verified by experimental data.

Though our work is limited by the number of simulated ions and applicable scope of the pseudo-potential approximation model, the result is still helpful for ion temperature measurement, sympathetic ion cooling efficiency improvement, and ion spatial configuration control.

References

[1] Diddams S A, Bergquist J C, Jefferts S R and Oates C W 2004 *Science* **306** 1318

[2] Bandi T, Affolderbach C, Calosso C E and Mileti G 2011 *Electron. Lett.* **47** 698

[3] Prestage J D and Weaver G L 2007 *Proc. IEEE* **95** 2235

[4] Semeghini G, Ferioli G, Masi L, Mazzinghi C, Wolswijk L, Minardi F, Modugno M, Modugno G, Inguscio M and Fattori M 2018 *Phys. Rev. Lett.* **120** 235301

[5] Van Eijkelenborg M A, Storkey M E, Segal D M and Thompson R C 1999 *Phys. Rev. A* **60** 3903

[6] Bowe P, Hornekær L, Brodersen C, Drewsen M and Hangst J S 1999 *Phys. Rev. A* **82** 2071

[7] Shang J J, Cui K F, Cao J, Wang S M, Chao S J, Shu H L and Huang X R 2016 *Chin. Phys. Lett.* **33** 103701

[8] Wu W B, Wu C W, Li J, Ou B Q, Xie Y, Wu W and Chen P X 2017 *Chin. Phys. B* **26** 080303

[9] Zuo Y N, Han J Z, Zhang J W and Wang L J 2019 *Appl. Phys. Lett.* **115** 061103

[10] Larson D J, Bergquist J C, Bollinger J J, Itano W M and Wineland D J 1986 *Phys. Rev. Lett.* **57** 70

[11] Mokhberi A and Willitsch S 2014 *Phys. Rev. A* **90** 023402

[12] Zhang C B, Offenberg D, Roth B, Wilson M A and Schiller S 2007 *Phys. Rev. A* **76** 012719

[13] Du L J, Chen T, Song H F, Chen S L, Li H X, Huang Y, Tong X, Gao K L and Guan H 2015 *Chin. Phys. B* **24** 083702

[14] Douglas D J, Frank A J and Mao D 2005 *Mass Spectrom. Rev.* **24** 1

[15] Kielpinski D, King B E, Myatt C J, Sackett C A, Turchette Q A, Itano W M, Monroe C, Wineland D J and Zurek W H 2000 *Phys. Rev. A* **61** 032310

[16] Verlet L 1967 *Phys. Rev.* **159** 98

[17] Verlet L 1968 *Phys. Rev.* **165** 201

[18] Zhang M Q and Skeel R D 1995 *J. Comput. Chem.* **16** 365

[19] Zhang J W, Wang S G, Miao K, Wang Z B and Wang L J 2014 *Appl. Phys. B* **114** 183

[20] Drakoudis A, Söllner M and Werth G 2006 *Int. J. Mass Spectrom.* **252** 61

[21] Berkeland D J, Miller J D, Bergquist J C, Itano W M and Wineland D J 1998 *J. Appl. Phys.* **83** 5025

[22] Bentine E, Foot C J and Trypogeorgos D 2020 *Comput. Phys. Commun.* **253** 10718

[23] Du L J, Song H F, Li H X, Chen S L, Chen T, Sun H Y, Huang Y, Tong X, Guan H and Gao K L 2015 *Chin. Phys. B* **24** 113703

[24] Leibfried D, Blatt R, Monroe C and Wineland D 2003 *Rev. Mod. Phys.* **75** 281

[25] Guggemos M, Heinrich D, Herrera-Sancho O A, Blatt R and Roos C F 2015 *New J. Phys.* **17** 103001

[26] Han J Z, Qin H R, Guo L M, Xin N C, Hu H X, Yu Y M, Dzuba V A, Zhang J W and Wang L J arXiv: 2002.04228 [physics.atom-ph]

[27] Blümel R, Chen J, Peik E, Quint W, Schleich W, Shen Y and Walther H 1988 *Nature* **334** 309

[28] Blümel R, Kappler C, Quint W and Walther H 1989 *Phys. Rev. A* **40** 808

[29] Xie Y, Wan W, Zhou F, Chen L, Li C H and Feng M 2012 *Chin. Phys. B* **21** 063201

[30] Han J Z, Qin H R, Xin N C, Hu H X, Yu Y M, Dzuba V A, Zhang J W and Wang L J 2021 *Appl. Phys. Lett.* **118** 101103